Sevoflurane Post-Conditioning Alleviated Hypoxic-Ischemic Brain Injury in Neonatal Rats by Inhibiting Endoplasmic Reticulum Stress-Mediated Autophagy via IRE1 Signalings

Jiayuan Niu
Shengjing Hospital of China Medical University
Ziyi Wu (1254757263@qq.com)
Shengjing Hospital of China Medical University https://orcid.org/0000-0001-5911-9127
Hang Xue
Shengjing Hospital of China Medical University
Yahan Zhang
Shengjing Hospital of China Medical University
Qiushi Gao
Shengjing Hospital of China Medical University
Chang Li
Shengjing Hospital of China Medical University
Ping Zhao
Shengjing Hospital of China Medical University

Research Article

Keywords: Sevoflurane post-conditioning, endoplasmic reticulum stress, autophagy, IRE1, hypoxic-ischemic brain injury

Posted Date: March 10th, 2021

DOI: https://doi.org/10.21203/rs.3.rs-274276/v1

Abstract

Post-conditioning with sevoflurane, a volatile anesthetic, has been proved to be neuroprotective against hypoxic-ischemic brain injury (HIBI). Our previous research showed that autophagy is over-activated in a rat model of neonatal HIBI, and inhibition of autophagy confers neuroprotection. There is increasing recognition that autophagy can be triggered by activating endoplasmic reticulum (ER) stress. This study aimed to explore: i) the relationship between ER stress and autophagy in the setting of neonatal HIBI; and ii) the possible roles of ER stress-mediated autophagy and IRE1 signalings in the neuroprotection of sevoflurane post-conditioning against neonatal HIBI. Seven-day-old rats underwent left common artery ligation followed by 2 h hypoxia (8% O2 / 92% N2). The relationship between ER stress and autophagy was examined by ER stress inducer (tunicamycin), ER stress inhibitor (4-PBA), or autophagy inhibitor (3-MA). Rats in the sevoflurane post-conditioning groups were treated with 2.4% sevoflurane for 30 min after HIBI induction. The roles of ER stress-mediated autophagy and the IRE1/JNK/beclin1 signaling pathway in the neuroprotection afforded by sevoflurane were examined by ER stress inducer (tunicamycin) and the IRE1 inhibitor (STF-083010). HIBI over-activated ER stress and autophagy in neonatal rats. HIBI-induced autophagy was significantly aggravated by tunicamycin but blocked by 4-PBA; however, HIBI-induced ER stress was not affected by 3-MA. Sevoflurane post-conditioning significantly alleviated ER stress, autophagy, cell apoptosis, and cognitive impairments, which were remarkably abolished by tunicamycin. Also, tunicamycin blocked sevoflurane-induced downregulation of IRE1/JNK/beclin1 signaling pathway. Whereas, IRE1 inhibitor could reverse the effects of tunicamycin. ER stress contributes to autophagy induced by HIBI. Furthermore, sevoflurane post-conditioning significantly protects against HIBI in neonatal rats by inhibiting ER stress-mediated autophagy via IRE1/JNK/beclin1 signaling pathway.

1. Introduction

Hypoxic-ischemic brain injury (HIBI) is a specific type of brain injury that result from oxygen deprivation and limited blood flow. HIBI remains one of the major causes of cerebral palsy and other neurodevelopmental disabilities in children, occurring in 1 to 8 per 1000 live births [1]. Although the benefit of therapeutic hypothermia has been shown, over 40% of the cooled infants still die or suffer moderate to severe disabilities [2]. In recent years, the use of medical gases as neuroprotective agents has gained great attention [3]. Sevoflurane is an inhaled anesthetic that is widely used in pediatric medicine and sevoflurane post-conditioning has been proven to protect against cerebral ischemia damage [3]. Thus, it is of high importance to evaluate the benefits of sevoflurane and the underlying molecular mechanisms.

Autophagy is an intracellular self-degradative process that is responsible for the removal of malformed proteins and damaged organelles in a lysosome-dependent manner. Our previous study showed that excessive autophagy is involved in cognitive impairments induced by HIBI in neonatal rats [4]. Growing evidence reveal that there is a crosstalk between autophagy and endoplasmic reticulum (ER) stress [5]. The ER is the cellular organelle that is responsible for protein folding and secretion, calcium homeostasis, and lipid biosynthesis. A wide variety of pathophysiologic and pharmacologic insults could disturb proper

ER function and thereby lead to an accumulation of misfolded and unfolded proteins in the ER, a condition termed as ER stress [6]. Study indicates that autophagy can be compensatorily activated to remove the accumulated dysfunctional proteins resulting from ER stress [7], hinting that ER stress might be a trigger for autophagy induction. Consequently, it is necessary to explore the relationship between ER stress and autophagy in the context of neonatal HIBI.

ER stress triggers an adaptive survival mechanism known as the unfolded protein response (UPR), which orchestrates the recovery of ER homeostasis by attenuating protein translation, enhancing degradation of misfolded proteins, and inducing ER-resident chaperones. The UPR consists of three main signaling systems initiated by three prototypical ER localized stress sensors: inositol-requiring enzyme 1 (IRE1), protein kinase RNA-like endoplasmic reticulum kinase (PERK), and activating transcription factor 6 (ATF6) [8]. During the ER stress, autophagy is suggested to be activated by three canonical branches of the UPR in distinctive manners. Particularly, in IRE1-deficient cells or cells treated with c-Jun N-terminal kinase (JNK) inhibitor, the autophagy induced by ER stress was inhibited, indicating that the IRE1-JNK pathway is required for autophagy activation after ER stress [9]. JNK activation leads to Bcl-2 phosphorylation and dissociation with beclin-1, a well-known key regulator of autophagy [10].

In this study, we explored the association between ER stress and autophagy in neonatal HIBI rats. Also, we evaluated the neuroprotective effects of sevoflurane post-conditioning targeting IRE1 signaling pathways between autophagy and ER stress at a molecular level.

2. Materials And Methods

2.1 Animals

Experiments were conducted on postnatal day 7 (P7) Sprague-Dawley rats in accordance with ethical approvals stipulated by the Animal Ethics Committee of Shengjing Hospital, China Medical University, Shenyang, China. Dams and their pups were housed under standard laboratory conditions under a 12 h light/dark cycle. Holding rooms were maintained at a constant temperature of 21–23°C and food and water were available ad libitum. Appropriate efforts were made to minimize the number of animals used and any potential suffering.

2.2 Experimental design

Experiment I: To evaluate the time course expression of ER stress marker GRP78 and autophagy marker LC3B after HIBI, rat pups (n = 32 animals per group) were randomly divided into two groups: Sham group and HI group. The left (ipsilateral) hippocampus was obtained from the brains of eight randomly selected pups from each group at each time point (3h, 6 h, 12 h, and 24 h post-HI) and were prepared for western blot.

Experiment II: To explore the association between ER stress and autophagy during HIBI, rat pups (n = 12 animals per group) were randomly assigned into five groups: Sham, HI, HI + TM (tunicamycin, ER stress

inducer), HI + 4-PBA (sodium 4-phenylbutyrate, ER stress inhibitor), and HI + 3-MA (3-methyladenine, autophagy inhibitor). The left (ipsilateral) hippocampus of six pups in each group were collected at 24 h post-HI for western blot. In addition, six rat pups in each group were sacrificed by transcardiac perfusion with phosphate-buffered solution (PBS) followed by 4% paraformaldehyde for brain section preparation at 24 h post-HI.

Experiment III: To evaluate the neuroprotective effects of sevoflurane post-conditioning that target IRE1 signaling pathways between autophagy and ER stress, rat pups (n = 22 animals per group) were randomly assigned into five groups: Sham, HI, SPC (sevoflurane post-conditioning), SPC + TM, and SPC + TM + IRE1 inhibitor. The left (ipsilateral) hippocampus of six pups in each group were collected at 24 h post-HI for western blot. Ten rats in each group were subjected to the open field and Morris water maze tests at P35 and P35–40, respectively. The six remaining rats from each group were used for Nissl stain.

2.3 Neonatal HIBI model, sevoflurane postconditioning, and drug administration

Seven-day-old rats were anesthetized using sevoflurane and subjected to permanent double ligation of the left common carotid artery using 7-0 surgical silk. The surgery was completed within five minutes. After waking, the pups were sent back to cages with their mothers for 2 h. The pups were then placed in a chamber ventilated with 8% O_2 and 92% N_2 at a flow rate of 2 L/min for 2 h. Rats in the sevoflurane groups inhaled 2.4% sevoflurane in a chamber with an atmosphere of 30% O_2 and 70% N_2 at a flow rate of 2 L/min for 30 min immediately after HI. Sham controls underwent anesthesia and skin incision only. In the Sham group, the chamber was ventilated with 30% O_2 and 70% N_2 at a flow rate of 2 L/min for 2 h.

The pups received an intracerebroventricular injection, which was performed at the left lateral ventricle. Tunicamycin (TM, 25 μM, 5 μL; Sigma-Aldrich, USA), sodium 4-phenylbutyrate (4-PBA, 200 μM, 5 μL; Sigma-Aldrich, USA), 3-methyladenine (3-MA, 10 μM, 5 μL; Proteintech, USA), or IRE1 inhibitor STF-083010 (50μM, 5 μL; MCE, China) was injected into left lateral ventricle 30 min before HI. Rats in the treatment groups that did not receive any drugs received the same volume of 0.1% DMSO alone.

2.4 Western blot analysis

The ipsilateral hippocampus was isolated and stored at -80℃ immediately until use. The samples were homogenized using RIPA lysis buffer and further centrifuged at 14,000 rpm at 4℃ for 30 min. The supernatant was collected and then the protein concentration was measured by the BCA Protein Assay Kit. An equivalent amount of protein samples was separated by SDS-PAGE gel electrophoresis and transferred to PVDF members. After blocking with 5% BSA, the membrane was incubated with the primary antibody overnight at 4°C. The primary antibodies were used with anti-GRP78 (1:500, Abcam, UK), anti-LC3B (1:500, Cell Signaling Technology, USA), p62 (1:500, Cell Signaling Technology, USA), IRE-1 (1:500, Abcam, UK), p-IRE-1 (1:500, Abcam, UK), JNK (1:500, Abcam, UK), p-JNK (1:500, Cell Signaling Technology, USA), beclin1 (1:500, Cell Signaling Technology, USA). Next day, the membranes were incubated with specific secondary anti-bodies for 2 h at room temperature. Immunolabeling was detected and photographed by GE Amersham Imager 600 using SuperSignal® West Pico Chemiluminescent

Substrate (Thermo Scientific, USA). Intensity of protein bands was quantified with Image J and normalized to that of β-actin.

2.5 TUNELassay

TUNEL staining was performed according to the manufacturer's instructions at 24 h after HI (in situ Apoptosis Detection Kit, Roche, Switzerland). Briefly, after dewaxing and heating in citrate buffer, sections were incubated for 30 min in blocking buffer (PBS containing 10% fetal bovine serum). Next, the sections were incubated with terminal deoxynucleotidyl transferase (TdT) and dUTP at 37℃ for 1 h. Nuclei were stained with DAPI. The fluorescence was captured using a Nikon Eclipse NI microscope and the number of TUNEL-positive cells was counted by Image J software. The results were presented as apoptosis index which was quantified as the ratio of (TUNEL-positive cells) / (total cells) × 100%.

2.6 Behavioral tests

The open field test was performed to assess locomotor and exploratory activities. Rats were placed individually in the center of a black plastic chamber (100 cm × 100 cm × 50 cm) over a period of 10 min. Tests were recorded and analyzed by EthoVision XT software (Noldus, Wageningen, The Netherlands). After each test, the arena was cleaned with 75% alcohol to avoid the presence of olfactory cues.

The Morris water maze tests were conducted to evaluate long-term learning and memory ability. The Morris water maze consisted of a circular black pool, 160 cm in diameter and 60 cm in depth, filled with water to a depth of 30 cm at room temperature (20 ± 1°C). A 12-cm-wide cylindrical platform was placed into the pool, 1.5 cm below the water surface and 30 cm from the wall. Extra-maze distal cues which had different colors and dimensions were suspended on the black curtains of the pool and were kept constant during the whole experiment. Training sessions lasted for five days and occurred four times a day with an interval of 30 min. Rats (n = 10 per group) were placed into the water facing the pool wall in one of four quadrants. Each rat was allowed 60 sec to search for the hidden platform. The daily order of entry into these quadrants was randomized. When the escape latency (time used to find the platform) was within 90 sec, the rats were made to stay on the platform for 20 sec. If the rats did not find the platform within 90 sec, they were guided to the platform on which they stayed for 20 sec and the escape latency was recorded as 90 sec. In spatial probe test, rats were put into the water and allowed to swim for 90 sec freely after the platform was removed. An automatic video camera system (Shanghai Mobiledatum Ltd, China) was set up above the pool to record every test.

2.7 Nissl staining

Coronal sections approximately 3.5 mm from caudal to bregma were obtained for Nissl staining. Representative microphotographs of the pyramidal cell layer of the CA1 region and CA3 region were captured using a digital microscope camera. Images of cells from three Nissl-stained sections were calculated in each rat. Numbers of healthy, Nissl-positive, neuronal cells were counted with Image J software.

2.8 Statistical analysis

GraphPad Prism Version 7.0 was used to perform all statistical analyses, and data are presented as mean ± standard deviation (SD). Comparisons between and within multiple groups were analyzed by one-way analysis of variance (ANOVA) followed by Student–Newman–Keuls post-hoc test. Data for escape latency were compared using two-way repeated measures ANOVA followed by Dunnett's multiple comparisons tests. Data for spatial probe test were compared using Dunn's multiple comparison test. A value of $p < 0.05$ was considered to be statistically significant.

3. Results

3.1 Expression levels of GRP78 and LC3 increased in time-dependent manner post HI

Firstly, ER stress and autophagy activity in the hippocampus were measured by western blot at different time points (3h, 6 h, 12 h, and 24 h) after HI. Glucose-regulated protein 78 (GRP78), also referred to as BiP, is a resident protein of the ER and upon ER stress, it first dissociates from ER membrane to help destroyed proteins refold and degrade [11]. Induction of GRP78 is considered as a marker for ER stress [12] and activation of autophagy was examined by immunoblotting of LC3B. As shown in Figure 1, GRP78 expression level was upregulated from 3 h to 24 h post-HI (Figure 1A, B, 3 h, $p < 0.05$; 6 h, $p < 0.01$; 12 h, $p < 0.05$; 24 h, $p < 0.05$) and the peak GRP78 level was observed at 6 h post-HI. Increase of LC3BII expression started at 6 h and reached a peak at 24 h (Figure 1A, C, 6 h: $p < 0.05$; 12 h: $p < 0.05$; 24 h: $p < 0.01$) after HI treatment. Our results indicated that both ER stress and autophagy are involved in the pathological process of neonatal HIBI. In addition, we chose HI-24 h model for the subsequent experiments.

3.2 ER stress triggered autophagy in the neonatal HIBI rats

Next, to determine the relationship between ER stress and autophagy in the context of neonatal HIBI, the rats were administrated with tunicamycin (ER stress inducer), 4-PBA (ER stress inhibitor), or 3-MA (autophagy inhibitor). p62 is a ubiquitin binding protein involved in selective autophagy and reduction of p62 has been regarded as a marker for increase of autophagic flux [13]. Results showed that HI insult over-activated ER stress and autophagy as indicated by upregulation of GRP78 (Figure 2A, B, $p < 0.05$ vs Sham group) and LC3BII (Figure 2A, C, $p < 0.01$ vs Sham group), and downregulation of p62 (Figure 2A, D, $p < 0.05$ vs Sham group). HI-induced ER stress and autophagy reinforced by combination with TM (Figure 2, GRP78: $p < 0.05$ vs HI group; LC3BII: $p < 0.05$ vs HI group; p62, $p < 0.05$ vs HI group), but counteracted by 4-PBA administration (Figure 2, GRP78: $p < 0.05$ vs HI group; LC3BII: $p < 0.05$ vs HI group; p62, $p < 0.05$ vs HI group). However, 3-MA was able to restrain autophagy activity (Figure 2, LC3BII: $p < 0.05$ vs HI group; p62: $p < 0.05$ vs HI group) without significant effects on ER stress (Figure 2, no significant difference in GRP78 expression). The above data indicated that ER stress was an upstream event of autophagy during neonatal HIBI.

3.3 ER stress-autophagy are involved in the cell apoptosis induced by HIBI

The cell apoptosis in the hippocampus was assessed by TUNEL assay. As illustrated in Figure 3, positive apoptosis cells were observed in HI group (CA1: $p < 0.01$ vs Sham group; CA3: $p < 0.01$ vs Sham group), and treatment with TM enhanced HI-induced apoptosis in the hippocampal CA1and CA3 subregions (CA1: $p < 0.05$ vs HI group; CA3: $p < 0.01$ vs HI group). Interfering ER stress by administration with 4-PBA restrained HI-induced cell apoptosis (CA1: $p < 0.05$ vs HI group; CA3: $p < 0.05$ vs HI group). Similarly, the autophagic inhibitor 3-MA suppressed HI-induced apoptosis via inhibition of autophagy (CA1: $p < 0.05$ vs HI group; CA3: $p < 0.05$ vs HI group).

3.4 Sevoflurane post-conditioning alleviated ER stress-mediated autophagy via regulation of the IRE1 pathway

Our previous researches indicated that sevoflurane-conferred neuroprotection against HIBI is related to inhibited excessive autophagy [14,15]. TM was applied in order to elucidate whether inhibition of autophagy by sevoflurane was mediated through suppressing ER stress. Sevoflurane post-conditioning attenuated HI-induced upregulation in GRP78 and LC3BII, and reduction in p62 (Figure 4A, B, HI vs. Sham: $p < 0.05$, $p < 0.01$, $p < 0.01$; SPC vs. HI: $p < 0.05$, $p < 0.05$, $p < 0.05$; for GRP78, LC3BII, and p62, respectively), but these effects were blocked by TM (Figure 4A, B, SPC + TM vs. SPC: $p < 0.05$, $p < 0.05$, $p < 0.05$ for GRP78, LC3BII, and p62, respectively).

Reports indicate that ER stress can trigger autophagy through IRE1 pathway [16]. The specific IRE1 inhibitor STF-083010 was administrated to further confirm that whether the IRE1/JNK/beclin1 pathway is involved in the neuroprotection of sevoflurane. Proteins in the IRE1 pathway, including p-IRE1/IRE1, p-JNK/JNK, and beclin1, were also assessed by Western blot. p-IRE1/IRE1, p-JNK/JNK ratio are used to stand for activation levels of IRE1 and JNK. IRE1 inhibitor reversed the effects of TM on the expression of GRP78, LC3BII, and p62 (Figure 4A, B, SPC+TM vs. SPC, $p < 0.05$, $p < 0.05$, $p < 0.05$; SPC+TM+IRE1 inhibitor vs. SPC+TM: $p < 0.05$, $p < 0.05$, $p < 0.05$; for GRP78, LC3BII, and p62, respectively), indicating that sevoflurane restrained ER stress-triggered autophagy through IRE1 pathway during HIBI. As presented in Figure 4, obvious increases in rations of p-IRE1/IRE1, p-JNK/JNK, and expression level of beclin1 were observed in ipsilateral hippocampus of rats compared with sham group (Figure 4C, D, HI vs. Sham: $p < 0.05$, $p < 0.05$, $p < 0.05$ for p-IRE1/IRE1, p-JNK/JNK, and beclin1, respectively). However, treatment with sevoflurane remarkably restrained the above changes (Figure 4C, D, SPC vs. HI: $p < 0.05$, $p < 0.05$, $p < 0.05$ for p-IRE1/IRE1, p-JNK/JNK, and beclin1, respectively), which were reversed by combination with TM (Figure 5, SPC+TM vs. SPC: $p < 0.05$, $p < 0.05$, $p < 0.05$ for p-IRE1/IRE1, p-JNK/JNK, and beclin1, respectively). IRE1 inhibitor counteracted the effects of TM (Figure 5, SPC+TM+IRE inhibitor vs. SPC+TM: $p < 0.05$, $p < 0.05$, $p < 0.05$ for p-IRE1/IRE1, p-JNK/JNK, and beclin1, respectively). The above results suggested that sevoflurane post-conditioning suppressed ER stress-autophagy via IRE1/JNK/beclin1 signaling pathway.

3.5 Sevoflurane post-conditioning improved cognitive performance and prevented neuronal loss in rats following HI

To evaluate locomotor activity and anxiety-like behavior in a novel environment, rats underwent the open field test at P35. As shown in Figure 5, no differences were observed among groups in total distance traveled, time spent in the center region, or the number of feces. These results suggested that treatment factors in this study did not influence locomotor activity or anxiety-like behavior in rats.

From day P35, Morris water maze tests were performed to evaluate spatial learning and memory. As shown in Figure 5, rats in all groups showed a significant downward trend in escape latency. Compared with the sham group, rats in the HI group exhibited longer escape latency to reach the platform (Figure 5D, day 29 post-HI, $p < 0.05$; day 30 post-HI, $p < 0.001$; day 31 post-HI, $p < 0.001$; day 32 post-HI, $p < 0.001$; day 33 post-HI, $p < 0.001$) and fewer platform crossings (Figure 5E, $p < 0.001$), indicating that rats displayed impaired learning and memory function following HIBI model. Sevoflurane post-conditioning successfully shortened escape latency (Figure 5D, day 30 post-HI, $p < 0.001$; day 31 post-HI, $p < 0.001$; day 32 post-HI, $p < 0.001$; day 33 post-HI, $p < 0.001$) and increased platform-crossing times (Figure 5E, $p < 0.05$), but these effects were reversed by TM (Figure 5 D, E, escape latency, day 30 post-HI, $p < 0.01$; day 31 post-HI, $p < 0.01$; day 32 post-HI, $p < 0.01$; day 33 post-HI, $p < 0.01$; platform crossing times, $p < 0.05$). However, treatment with IRE1 inhibitor blocked the negative effects of TM (Figure 5 D, E, escape latency, day 31 post-HI, $p < 0.01$; day 32 post-HI, $p < 0.01$; day 33 post-HI, $p < 0.01$; platform crossing times, $p < 0.05$).

Nissl staining procedures were conducted to determine neuron status among groups after behavioral tests. Neurons with increased intracellular space were scattered in an irregular arrangement in the hippocampus of the rats in the HI and SPC +TM groups, whereas neurons in the SPC and SPC + IRE1 inhibitor groups preserved a better functional status. Sevoflurane significantly attenuated HI-induced reduction of neuronal density in the CA1 and CA3 hippocampal areas (HI vs. Sham: $p < 0.001$, $p < 0.001$; SPC vs. HI: $p < 0.001$, $p < 0.001$; for CA1 and CA3, respectively). Treatment with TM increased neuronal density in the hippocampus (SPC+TM vs. SPC: $p < 0.001$, $p < 0.001$ for CA1 and CA3, respectively), while IRE1 inhibitor blocked the effects of TM (SPC+TM+IRE1 inhibitor vs. SPC+TM: $p < 0.001$, $p < 0.01$ for CA1 and CA3, respectively).

These results indicated that sevoflurane post-conditioning alleviated HI-induced cognitive impairments, possibly by regulating ER stress-mediated autophagy via IRE1 signaling pathway.

4. Discussion

HIBI is one of the major causes of neonatal mortality and could cause neurodevelopmental disabilities, with limited therapy options. Excessive autophagy caused by HIBI may cause neuronal death [4]. Our previous studies revealed that the volatile anesthetic sevoflurane could exert neuroprotective effects against HIBI via autophagy inhibition [14,15]. Yet, the underlying mechanisms have not be fully understood. The present study provided evidence that ER stress contributed to autophagy in HIBI neonatal rats. In addition, sevoflurane post-conditioning alleviated ER stress-dependent autophagy via regulating IRE1/JNK/beclin1 pathways.

Autophagy is one of the pathogenetic mechanisms of hypoxic-ischemic cerebral injury [4,17]. Autophagy occurs constitutively at a basal level to maintain cellular homeostasis and function, but can also be induced by both physiological and pathological stimuli. Our previous study revealed that in neonatal rat HIBI model, when over-activated autophagy is induced by HI insult, it is deleterious and contributes to neuronal apoptosis and cognitive dysfunction [4]. It is becoming increasingly clear that ER stress is one of the signaling pathways involved in regulation of autophagy [18,5]. GRP78 is a central regulator of the ER stress signaling pathway with established function as an ER chaperone protein. Upon ER stress, it first dissociates from ER membrane to help destroyed proteins refold and degrade [12]. Thus, induction of GRP78 is considered as a marker for ER stress. In the present study, both ER stress and autophagy are activated in the pathological process of neonatal HIBI, as evidenced by increased GRP78 and LC3BII expression, as well as decreased p62 expression. Our results supported results from previous studies that ER stress and autophagy are involved in ischemic stroke [19,20]. Of note, to determine the relationship between ER stress and autophagy in the setting of neonatal HIBI, the rats were administrated with TM (ER stress inducer), 4-PBA (ER stress inhibitor), or 3-MA (autophagy inhibitor). Results showed that HIBI-induced autophagy was significantly enhanced by TM but counteracted by 4-PBA; however, HIBI-induced ER stress was not affected by 3-MA. The above data suggested that ER stress is also a potent trigger for autophagy in neonatal HIBI rats. Similarly, ER stress mediated-autophagy has been implicated in the pathogenesis of traumatic brain injury [21].

A number of studies have demonstrated that sevoflurane post-conditioning exhibits neuroprotective effects against HIBI, and the protective mechanisms may be attributed to its suppressing autophagy properties. Since ER stress is the upstream pathway inducing autophagy in HIBI, we hypothesized that sevoflurane restrained autophagy through inhibiting ER stress. To confirm this hypothesis, ER stress inductor TM was administrated. In the present study, there were significant decreases in GRP78 and LC3BII protein levels, whereas increase in p62 protein level following sevoflurane post-conditioning, but these effects were blocked by TM. Alteration of the protein expressions mentioned above revealed that sevoflurane restrained autophagy through inhibiting ER stress.

Our results also suggested that the IRE1/JNK/beclin1 pathway was involved in the mechanisms of neuroprotection of sevoflurane during the inhibition of ER stress-induced autophagy. The UPR is an adaptive pathway that aims to reestablish cellular homeostasis after ER stress. When the UPR occurs, three ER-resident transmembrane proteins (IRE1, PERK and ATF6) sense it through a luminal domain and transmits to the cytoplasm and nucleus in order to facilitate protein folding, translational attenuation and ER-associated degradation of misfolded proteins [22]. Interestingly, in a study of IRE1-PERK-ATF6-deficiency in ER stress, autophagy was suppressed in the IRE1 signaling pathway, but not in the PERK and ATF6 pathways [9]. In embryonic fibroblasts, a defect of IRE1 decreases the accumulation of LC3-positive vesicles [23]. Under physiological conditions, the ER chaperone GRP78 binds to the regulatory luminal domain of IRE1 and suppresses its activity, whereas during ER stress, GRP78 dissociates from IRE1, allowing it to oligomerize, trans-autophosphorylate, and subsequently activate its endoribonuclease domain [24]. As expected, p-IRE1/IRE1 ratio was increased with HIBI-induced ER stress but decreased by sevoflurane. It has been reported that ER stress-induced autophagy is regulated through IRE1 interaction

with TRAF2 to mediate JNK activation/phosphorylation [9]. Previous studies have also further revealed that elevated JNK signaling is associated with autophagy induction [25]. One of the key checkpoints in the modulation of autophagy is the interaction between the autophagic effector beclin-1 and the members of the anti-apoptotic Bcl-2 family [26]. JNK activation induced phosphorylation of Bcl-2 and disrupts the formation of Bcl-2/beclin-1 autophagy suppressor complexes [27,28]. Western blot analysis showed that sevoflurane significantly inhibited HI-induced the upregulation of p-IRE1/IRE1, p-JNK/JNK, and beclin-1. TM reversed the effects of sevoflurane on IRE1/JNK/beclin-1 signaling and the autophagy markers LC3B-II and beclin1, and IRE1 inhibitor counteracted the effects of TM. Therefore, the mechanisms by which sevoflurane affects the ER stress-induced autophagy are attributed to the inhibited of IRE1/JNK/beclin-1 (Figure 7).

In summary, our results have shed some light on the mechanisms of sevoflurane in treatment for HIBI. Our results showed that the ER stress-autophagy signaling is a crucial mechanistic event involved in HIBI, and sevoflurane post-conditioning significantly protects against HIBI in neonatal rats by inhibiting ER stress-mediated autophagy via IRE1/JNK/beclin1 signaling pathway.

Declarations

Funding

This work was supported by the National Nature Science Foundation of China (No.81870838), Liaoning Province Distinguished Professor Support Program (No. XLYC1802096), Shenyang Clinical Medicine Research Center of Anesthesiology (No. 19-110-4-24, No. 20-204-4-44), and the Outstanding Scientific Fund of Shengjing Hospital (No. 201708).

Author contributions

J.-Y. N. and P. Z. conceived and designed experiments. J.-Y. N., H. X., Q-S. G., Y.-H. Z. and C. L. performed experiments, generated and analyzed the data. Z.-Y. W. wrote the manuscript with the help of P. Z. All authors read and approved the final manuscript.

Data availability statement

The data that support the findings of this study are available from the corresponding author upon reasonable request.

Compliance with Ethical Standards

Conflict of Interest

The authors declare that they have no conflicts of interest.

References

1. Douglas-Escobar M, Weiss MD (2015) Hypoxic-ischemic encephalopathy: a review for the clinician. JAMA pediatrics 169(4):397–403. doi:10.1001/jamapediatrics.2014.3269
2. Edwards AD, Brocklehurst P, Gunn AJ, Halliday H, Juszczak E, Levene M, Strohm B, Thoresen M, Whitelaw A, Azzopardi D (2010) Neurological outcomes at 18 months of age after moderate hypothermia for perinatal hypoxic ischaemic encephalopathy: synthesis and meta-analysis of trial data. BMJ 340:c363. doi:10.1136/bmj.c363
3. Wang YZ, Li TT, Cao HL, Yang WC (2019) Recent advances in the neuroprotective effects of medical gases. Medical gas research 9(2):80–87. doi:10.4103/2045-9912.260649
4. Xu Y, Tian Y, Tian Y, Li X, Zhao P (2016) Autophagy activation involved in hypoxic-ischemic brain injury induces cognitive and memory impairment in neonatal rats. Journal of neurochemistry 139(5):795–805. doi:10.1111/jnc.13851
5. Qi Z, Chen L (2019) Endoplasmic Reticulum Stress and Autophagy. Adv Exp Med Biol 1206:167–177. doi:10.1007/978-981-15-0602-4_8
6. Kaneko M, Imaizumi K, Saito A, Kanemoto S, Asada R, Matsuhisa K, Ohtake Y (2017) ER Stress and Disease: Toward Prevention and Treatment. Biol Pharm Bull 40(9):1337–1343. doi:10.1248/bpb.b17-00342
7. Ding WX, Yin XM (2008) Sorting, recognition and activation of the misfolded protein degradation pathways through macroautophagy and the proteasome. Autophagy 4(2):141–150. doi:10.4161/auto.5190
8. Lai E, Teodoro T, Volchuk A (2007) Endoplasmic Reticulum Stress: Signaling the Unfolded Protein Response. Physiology 22(3):193–201. doi:10.1152/physiol.00050.2006
9. Ogata M, Hino S, Saito A, Morikawa K, Kondo S, Kanemoto S, Murakami T, Taniguchi M, Tanii I, Yoshinaga K, Shiosaka S, Hammarback JA, Urano F, Imaizumi K (2006) Autophagy is activated for cell survival after endoplasmic reticulum stress. Molecular cellular biology 26(24):9220–9231. doi:10.1128/mcb.01453-06
10. Lorin S, Pierron G, Ryan KM, Codogno P, Djavaheri-Mergny M (2010) Evidence for the interplay between JNK and p53-DRAM signalling pathways in the regulation of autophagy. Autophagy 6(1):153–154. doi:10.4161/auto.6.1.10537
11. Feng J, Chen Y, Lu B, Sun X, Zhu H, Sun X (2019) Autophagy activated via GRP78 to alleviate endoplasmic reticulum stress for cell survival in blue light-mediated damage of A2E-laden RPEs. BMC Ophthalmology 19(1):249. doi:10.1186/s12886-019-1261-4
12. Lee AS (2005) The ER chaperone and signaling regulator GRP78/BiP as a monitor of endoplasmic reticulum stress. Methods 35(4):373–381. doi:10.1016/j.ymeth.2004.10.010
13. Mathew R, Karp CM, Beaudoin B, Vuong N, Chen G, Chen HY, Bray K, Reddy A, Bhanot G, Gelinas C, Dipaola RS, Karantza-Wadsworth V, White E (2009) Autophagy suppresses tumorigenesis through elimination of p62. Cell 137(6):1062–1075. doi:10.1016/j.cell.2009.03.048
14. Wang S, Xue H, Xu Y, Niu J, Zhao P (2019) Sevoflurane Postconditioning Inhibits Autophagy Through Activation of the Extracellular Signal-Regulated Kinase Cascade, Alleviating Hypoxic-Ischemic Brain

Injury in Neonatal Rats. Neurochem Res 44(2):347–356. doi:10.1007/s11064-018-2682-9

15. Xue H, Xu Y, Wang S, Wu ZY, Li XY, Zhang YH, Niu JY, Gao QS, Zhao P (2019) Sevoflurane post-conditioning alleviates neonatal rat hypoxic-ischemic cerebral injury via Ezh2-regulated autophagy. Drug Des Devel Ther 13:1691–1706. doi:10.2147/dddt.s197325
16. Lee H, Noh J-Y, Oh Y, Kim Y, Chang J-W, Chung C-W, Lee S-T, Kim M, Ryu H, Jung Y-K (2011) IRE1 plays an essential role in ER stress-mediated aggregation of mutant huntingtin via the inhibition of autophagy flux. Hum Mol Genet 21(1):101–114. doi:10.1093/hmg/ddr445
17. Lu Q, Harris VA, Kumar S, Mansour HM, Black SM (2015) Autophagy in neonatal hypoxia ischemic brain is associated with oxidative stress. Redox Biology 6:516–523. doi:https://doi.org/10.1016/j.redox.2015.06.016
18. Yorimitsu T, Klionsky DJ (2007) Endoplasmic reticulum stress: a new pathway to induce autophagy. Autophagy 3(2):160–162. doi:10.4161/auto.3653
19. Chi L, Jiao D, Nan G, Yuan H, Shen J, Gao Y (2019) miR-9-5p attenuates ischemic stroke through targeting ERMP1-mediated endoplasmic reticulum stress. Acta Histochem 121(8):151438. doi:https://doi.org/10.1016/j.acthis.2019.08.005
20. Wang P, Shao BZ, Deng Z, Chen S, Yue Z, Miao CY (2018) Autophagy in ischemic stroke. Progress in neurobiology 163–164:98–117. doi:10.1016/j.pneurobio.2018.01.001
21. Wang D-Y, Hong M-Y, Pei J, Gao Y-H, Zheng Y, Xu X (2021) ER stress mediated–autophagy contributes to neurological dysfunction in traumatic brain injury via the ATF6 UPR signaling pathway. Mol Med Rep 23 (4). doi:10.3892/mmr.2021.11886
22. Adams CJ, Kopp MC, Larburu N, Nowak PR, Ali MMU (2019) Structure and Molecular Mechanism of ER Stress Signaling by the Unfolded Protein Response Signal Activator IRE1. Frontiers in Molecular Biosciences 6 (11). doi:10.3389/fmolb.2019.00011
23. Høyer-Hansen M, Jäättelä M (2007) Connecting endoplasmic reticulum stress to autophagy by unfolded protein response and calcium. Cell death differentiation 14(9):1576–1582. doi:10.1038/sj.cdd.4402200
24. Pfaffenbach KT, Lee AS (2011) The critical role of GRP78 in physiologic and pathologic stress. Curr Opin Cell Biol 23(2):150–156. doi:https://doi.org/10.1016/j.ceb.2010.09.007
25. Zhang Y, Chen P, Hong H, Wang L, Zhou Y, Lang Y (2017) JNK pathway mediates curcumin-induced apoptosis and autophagy in osteosarcoma MG63 cells. Experimental therapeutic medicine 14(1):593–599. doi:10.3892/etm.2017.4529
26. Xu HD, Qin ZH (2019) Beclin 1, Bcl-2 and Autophagy. Adv Exp Med Biol 1206:109–126. doi:10.1007/978-981-15-0602-4_5
27. He C, Zhu H, Li H, Zou M-H, Xie Z (2013) Dissociation of Bcl-2–Beclin1 Complex by Activated AMPK Enhances Cardiac Autophagy and Protects Against Cardiomyocyte Apoptosis in Diabetes. Diabetes 62(4):1270–1281. doi:10.2337/db12-0533
28. Wei Y, Pattingre S, Sinha S, Bassik M, Levine B (2008) JNK1-Mediated Phosphorylation of Bcl-2 Regulates Starvation-Induced Autophagy. Mol Cell 30(6):678–688.

doi:https://doi.org/10.1016/j.molcel.2008.06.001

Figures

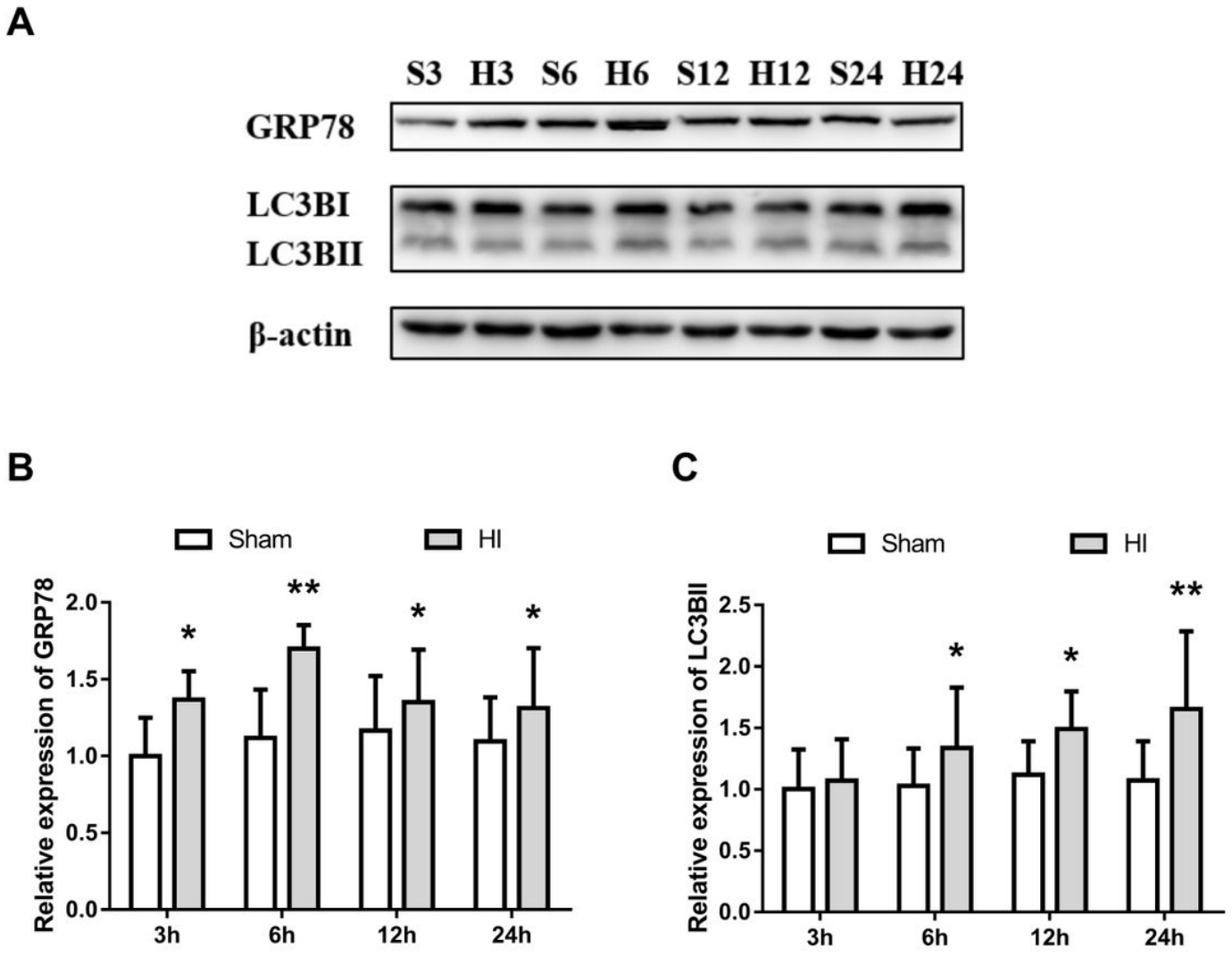

Figure 1

Temporal expression of GRP78 and LC3BII in the ipsilateral hippocampus after HIBI. Levels of GRP78 and LC3BII in the ipsilateral hippocampus were evaluated with Western blot at 3, 6, 12, and 24 h post-HI. (A) Representative pictures of Western blot data. (B) The relative value of band density was measured with Image J and normalized to that of β-actin. Data were presented as mean ± SD. n = 8 for each group. *$p < 0.05$ and **$p < 0.01$ compared with sham group.

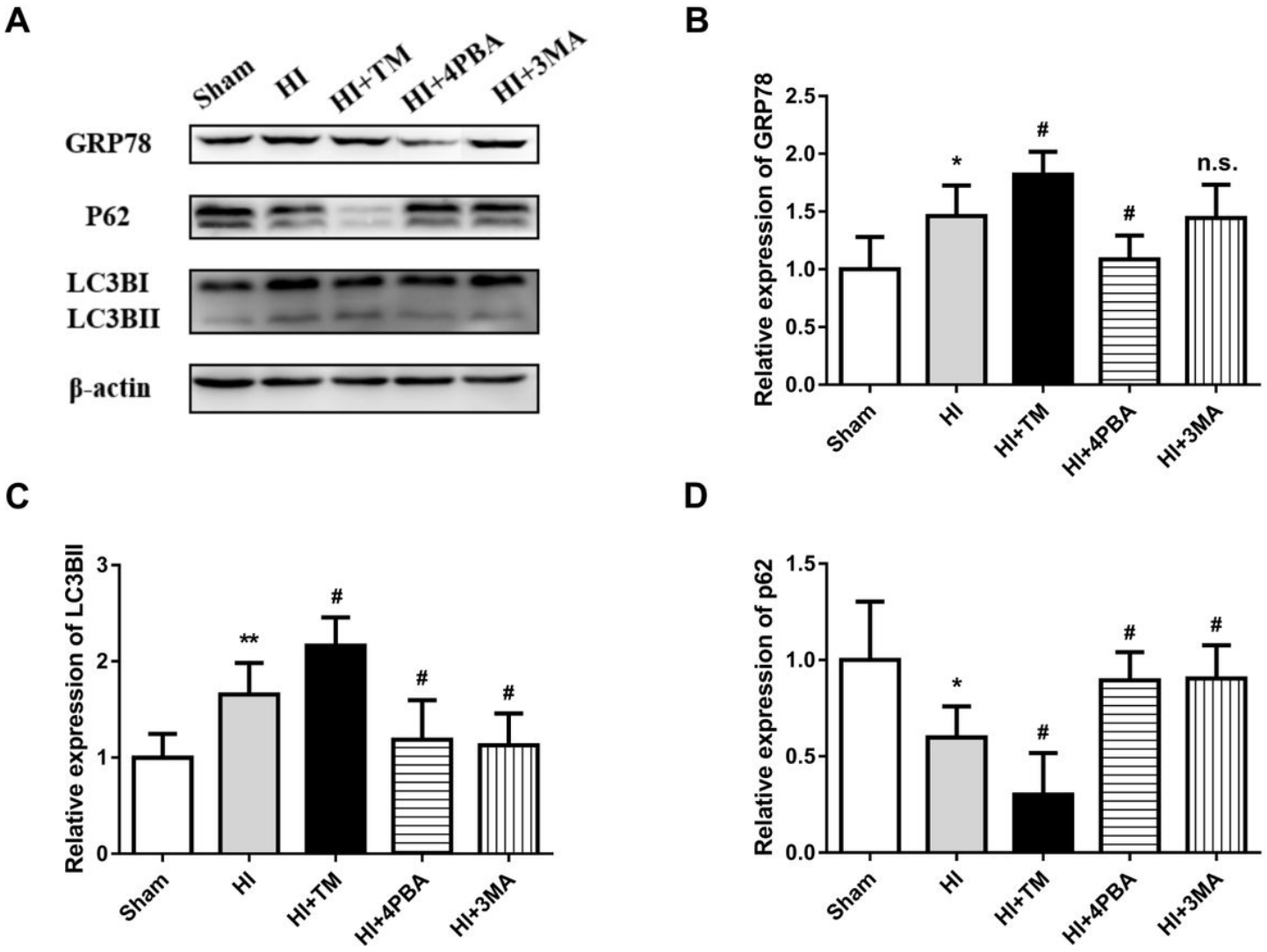

Figure 2

ER stress triggered autophagy in the neonatal HIBI rats. (A) Representative Western blot results of GRP78, LC3B, and p62 were shown. (B) The relative value of band density was measured with Image J and normalized to that of β-actin. Data were presented as mean ± SD. n = 6 for each group. *p < 0.05 and **p < 0.01 compared with Sham group. #p < 0.05 compared with HI group.

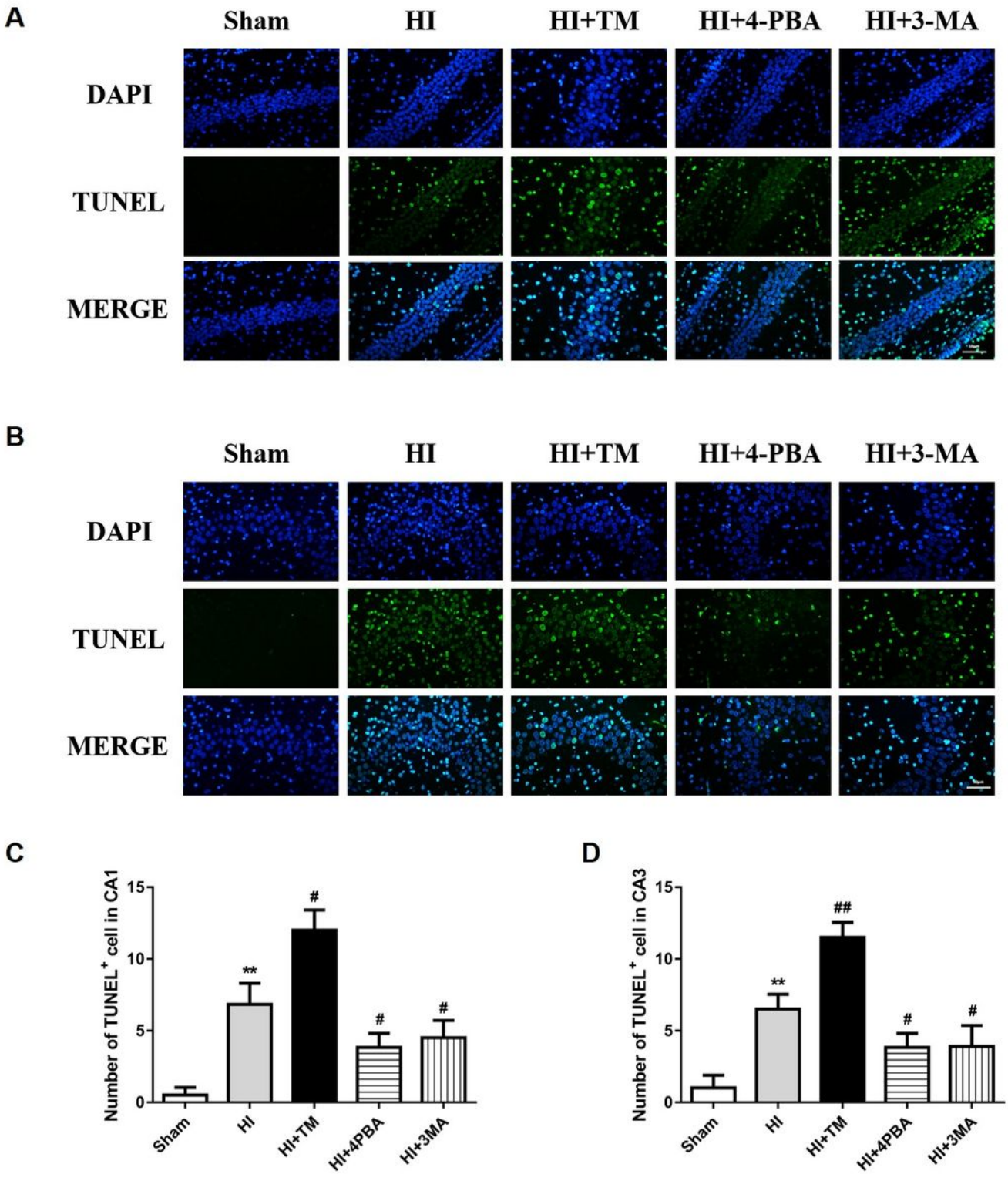

Figure 3

ER stress-autophagy are involved in the cell apoptosis induced by HIBI. (A-B) TUNEL assay was performed to detect apoptosis, and the representative images were shown. Green: apoptotic cells. Blue: nucleus. Scale bar = 50 μm. (C-D) Apoptosis index was expressed as the ratio of (apoptotic cells)/(total cells)×100%. n = 6 for each group. **p < 0.01 compared with Sham group. #p < 0.05 and ##p < 0.01 compared with HI group.

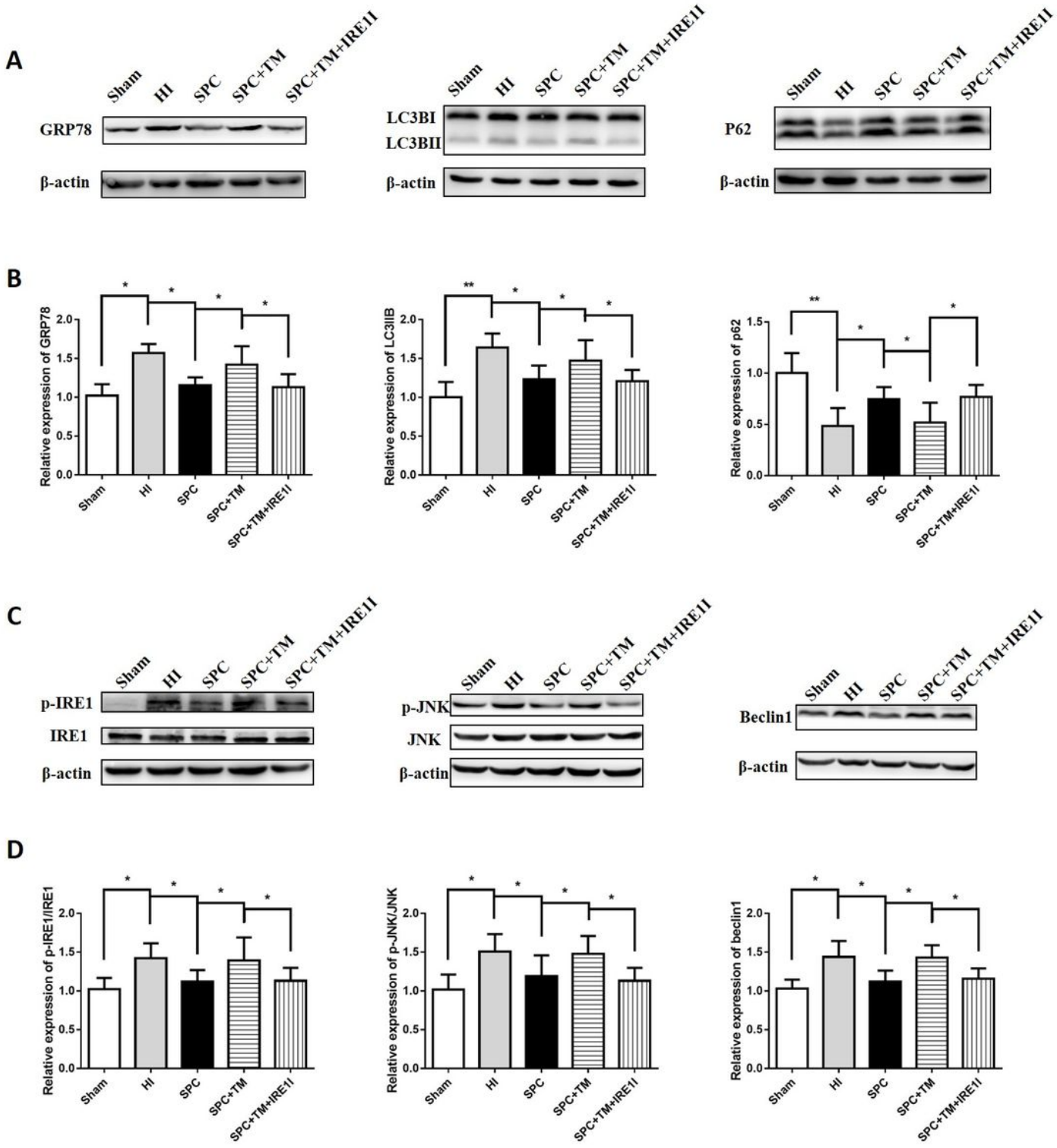

Figure 4

Sevoflurane post-conditioning suppressed ER stress-dependent autophagy via regulating IRE1 pathway. (A) Representative Western blot results of GRP78, LC3B, and p62 were shown. (B) Relative band density was measured with Image J and normalized to that of β-actin. (C) Representative Western blot results of p-IRE1/IRE1, p-JNK/JNK, and beclin1 were shown. (D) Relative band density was measured with Image J

and normalized to that of β-actin. Data were presented as mean ± SD. n = 6 for each group. *p < 0.05 and **p < 0.01 compared with the indicated group.

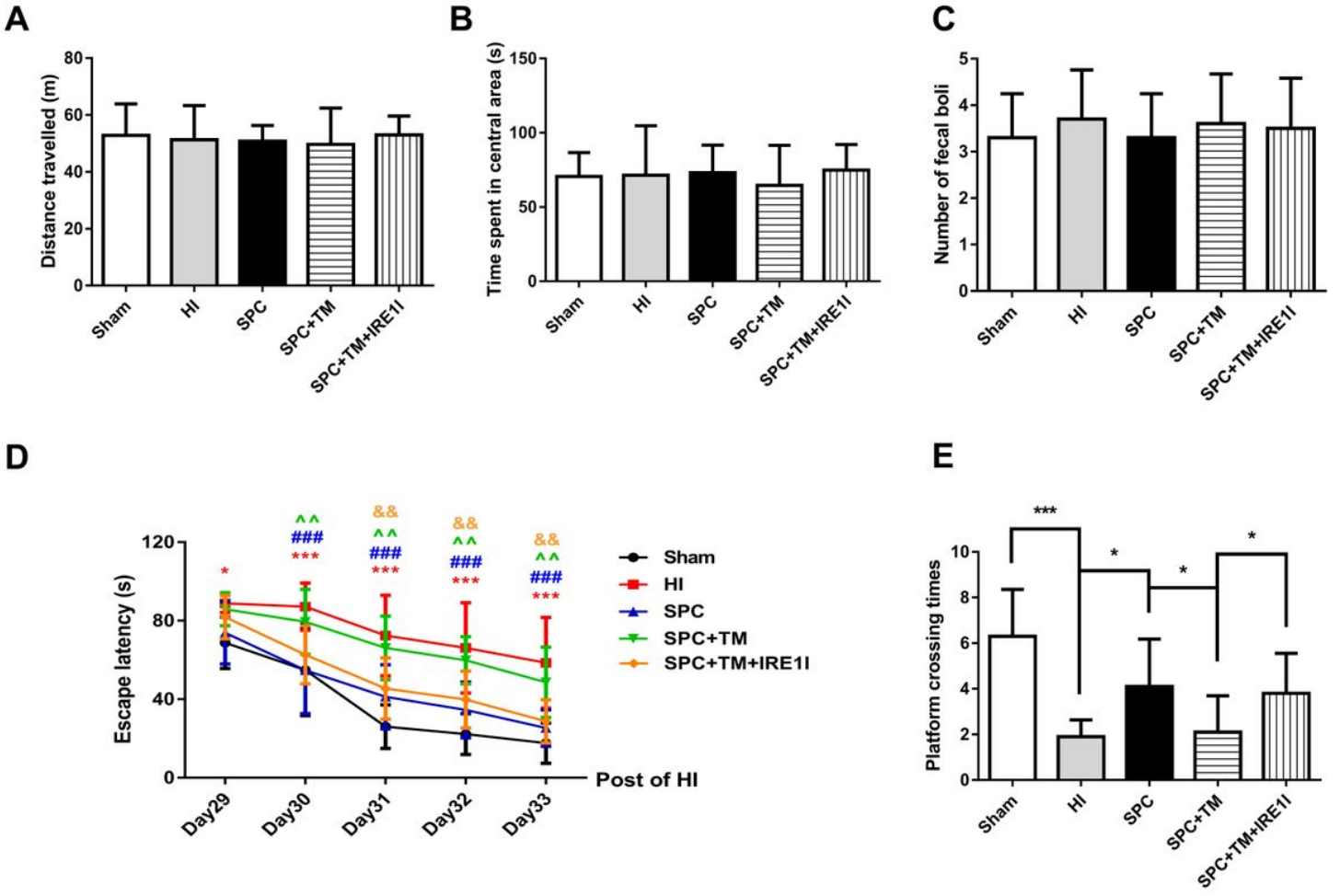

Figure 5

Evaluation of rats' behavior in the open field test (OFT) and the Morris water maze (MWM) tests during the adolescent phase. (A) Total distance traveled in the OFT. (B) Time spent in the central area of the OFT. (C) The number of fecal pellets in the OFT. (D) Escape latency in the MWM tests. (E) Platform crossing time in the MWM tests. Data were presented as mean ± SD. n = 10 for each group. In Figure 5D, *p < 0.05 and ***p < 0.001 compared with Sham group. ###p < 0.001 compared with HI group. ^^p < 0.01 compared with SPC group. &&p < 0.01 compared with SPC+TM group. In Figure 5E, *p < 0.05 and ***p < 0.001 compared with the indicated group.

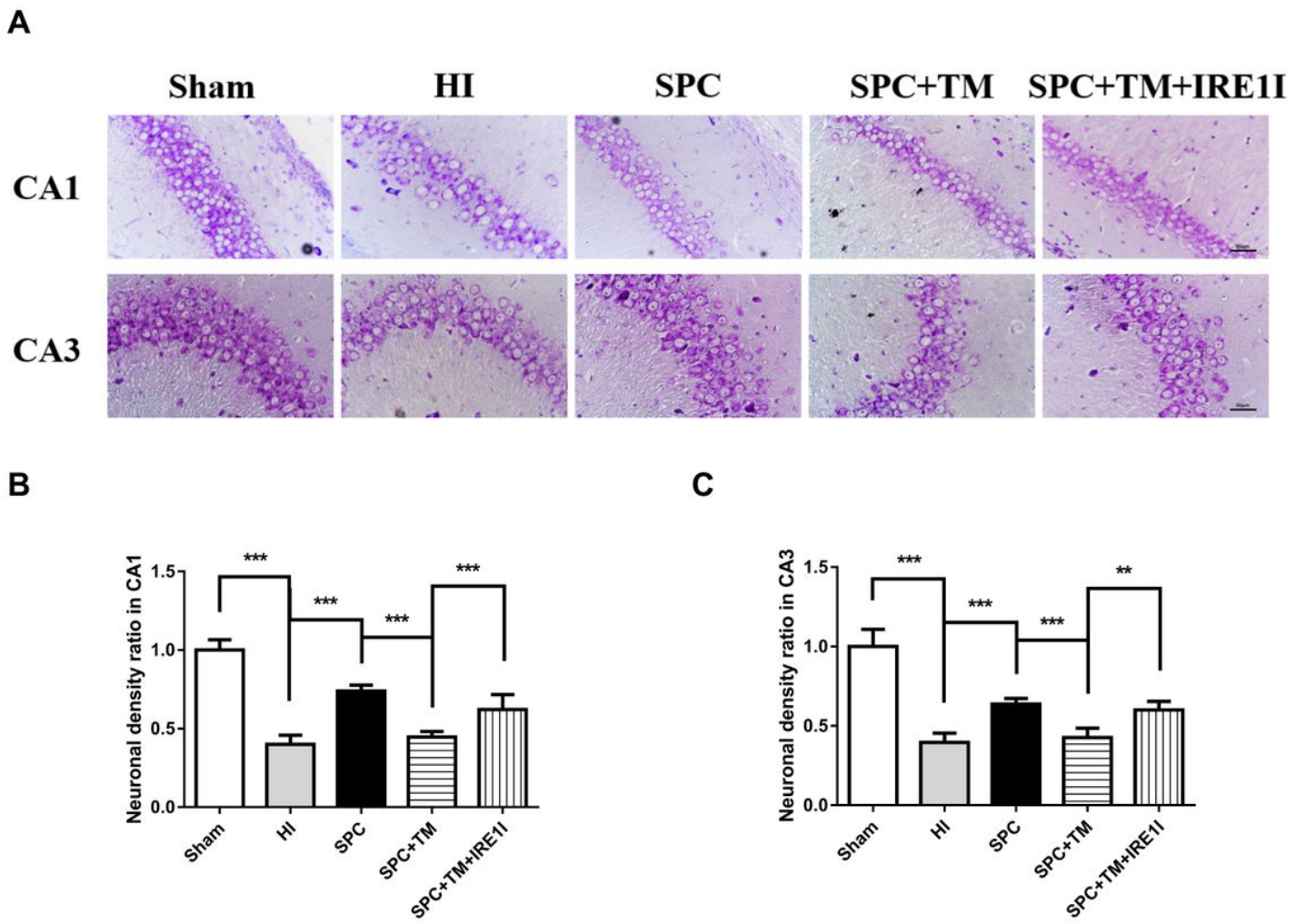

Figure 6

Evaluation of hippocampal neuronal cells in newborn rats with HIBI. (A) Histological Nissl staining in CA1 and CA3 regions of hippocampus. Scale bar = 50μm. (B) Neuronal density ratio in CA1 region of hippocampus. (C) Neuronal density ratio in CA3 region of hippocampus. Data were presented as mean ± SD. n = 6 for each group. **p < 0.01 and ***p < 0.001 compared with the indicated group.

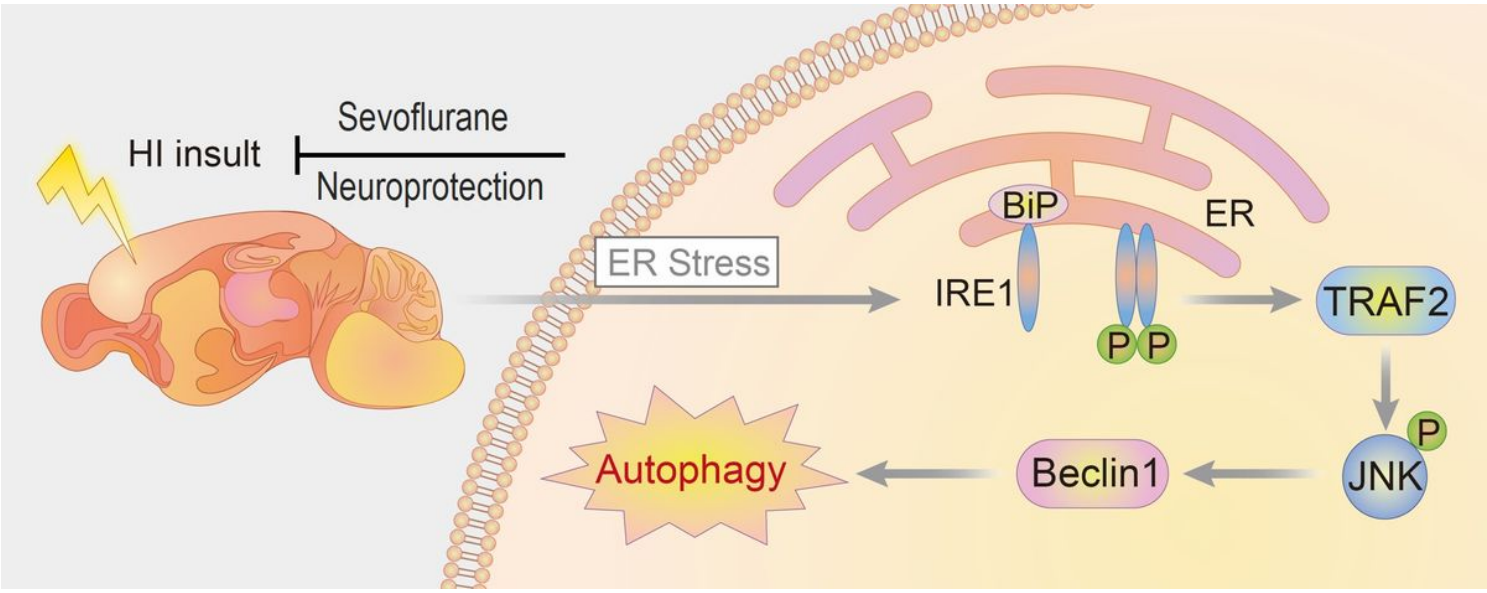

Figure 7

Mechanisms underlying the protective effects of sevoflurane post-conditioning against neonatal hypoxic-ischemic brain injury.